IEEE Access
Multidisciplinary | Rapid Review | Open Access Journal

Received April 9, 2018, accepted May 4, 2018, date of publication June 5, 2018, date of current version July 6, 2018.

Digital Object Identifier 10.1109/ACCESS.2018.2834565

Automotive ABS/DYC Coordinated Control Under Complex Driving Conditions

ZHENPO WANG, JUNJUN ZHU, LEI ZHANG, (Member, IEEE), AND YACHAO WANG

Collaborative Innovation Center for Electric Vehicles in Beijing, National Engineering Laboratory for Electric Vehicles, Beijing Institute of Technology, Beijing 100081, China

Corresponding author: Lei Zhang (lei_zhang@bit.edu.cn)

This work was supported by the Ministry of Science and Technology of the People's Republic of China under Grant 2017YFB0103600.

ABSTRACT This paper presents an antilock braking system/direct yaw-moment control (ABS/DYC) coordinated control scheme in order to shorten the braking distance while ensuring the vehicle stability during emergency braking under complex driving conditions. Particularly, the braking actuator failure and driving on low-μ and μ-split roads are considered. The proposed control scheme is composed of three cascaded controllers. The first-level controller is used to derive and trace the desired yaw rate for DYC control based on the driver's intent, exert conventional ABS control to maximize the braking force without considering braking actuator fault occurrence, and synthesize constraint conditions such as braking actuator failure and so forth. The second-level controller is used to determine on which side to fully capitalize for the maximum tire/road adhesion utilization. The third-level controller is leveraged to realize optimal torque allocation to each actuation motor with the purpose of minimizing the tire load. The effectiveness of the proposed ABS/DYC coordinated control scheme is verified through both simulation and hardware-in-loop experimentation.

INDEX TERMS ABS/DYC coordinated control, anti-lock braking system (ABS), braking force allocation, direct yaw-moment control (DYC).

I. INTRODUCTION

With the ever-increasing number of ground vehicles being used in modern society, transportation electrification and automotive safety have attracted enormous attention. Vehicle stability control (VSC) has been the focus of intensive research in order to enhance vehicle stability and prevent fatal car accidents [1]. Substantial progress has been made in VSC over past decades, and the vehicle anti-lock braking system (ABS) and electronic stability control (ESC) are two representative achievements in this regard [4]. Generally, ABS can adjust the braking force according to the tire/road adhesion conditions, prevent the tire locking and decrease the braking distance [5]. ESC is able to help vehicle stabilization by executing differential braking/driving, i.e., applying different braking/driving torques to each wheel, to generate an additional yaw-moment [6]. In this sense, ESC is equal to the direct yaw-moment control (DYC). Additionally, active front steering (AFS) is also an effective tool for ESC, and its integration with DYC can possibly yield better effects than the independent execution of either [7].

Since the widespread adoption of ABS in mass production cars in 1978, a plethora of methods for elevating ABS control performance have been presented in the literature, which can be roughly grouped into two categories, i.e., rule- and model-based methods. The rule-based methods are dominant in modern commercial vehicles due to its ease of implementation and high reliability. Hereinto, the logic threshold method exemplifies a rule-based ABS control technique, where the braking pressure at each wheel can be controlled within a certain range through tire slip ratio regulation. For instance, Lu *et al.* [8] devised a fuzzy-logic controller for ABS control and verified its performance through the Adams/Car virtual experimentation. Similarly, based on fuzzy control, Yang *et al.* [9] proposed a fuzzy-PID ABS control strategy, in which the tire slip ratio is controlled by a PID controller with its controller parameters tuned by the fuzzy controller. Fargione *et al.* [10] further optimized the membership function of the conventional ABS fuzzy controller with the genetic algorithms (GAs) to improve its control performance under various driving conditions. Köppena *et al.* [11] proposed a threshold adaptive method based on the perturbation theory for ABS control, which was verified to be superior to the traditional threshold method. In spite of the widespread use of rule-based methods, their control effect relies heavily on the

experience of engineers and is lack of optimality; this may notably curtail the ABS performance. In order to improve the ABS performance, model-based control approaches have emerged in recent years. For instance, Zhang *et al.* [12] put forward a novel method by estimating the tire/road friction coefficient and then designed a sliding-mode controller (SMC) to trace the optimal slip ratio. Du *et al.* [13] developed an ABS control strategy based on model predict control (MPC) for hybrid electric vehicles.

The aim of ESC is to realize the driver's intent while ensuring vehicle lateral stability. Conventionally, there are two means to realize ESC of the vehicle, i.e., by the active front steering (AFS) system and/or direct yaw-moment control. The coordination of ABS control and ESC with either AFS or DYC has enormous potential for promoting vehicle stability under emergency braking scenarios, and thus solicits attention from both academia and industry practitioners [14]. For instance, Tjønnås and Johansen [15] synthesized a PI controller to derive the required yaw moment, and decomposed it to the required braking force at each wheel and the steering angle with an optimal allocation strategy. Choi *et al.* [16] proposed a method to coordinate the AFS and DYC based on model predictive control (MPC). Wu *et al.* [17] propose a human-machine-cooperative-driving controller with a hierarchical structure for vehicle dynamic stabilization by introducing a coordination factor to regulate AFS and DYC. Other research results also prove that the AFS yields good performance in ESC control but at the expense of high cost [7], [18], [19]. Moreover, it has some limitations when a large steering angle is anticipated. In contrast, the DYC can compensate the aforementioned drawbacks, and exhibits potential to coordinate with ABS to improve the vehicle stability during emergency braking maneuvers, especially under urgent steering and complex driving conditions.

Both ABS and DYC can be realized by independently controlling the braking force at each wheel. Nevertheless, their control targets are conflicting, and this becomes more troublesome under some complex driving conditions. For example, when braking on a μ-split road with dissimilar tire/road friction coefficients on both wheel tracks, there would be significant braking force imbalance if ABS tries to fully capitalize on the road friction on the left and right tracks at the same time. In such case, low selection control (LSC) is usually used to solve this dilemma, where the braking pressures at wheels with the same axle is kept the same and the lower braking force is selected as the communal control target for all braking actuators. Inevitably, this sacrifices some braking force so as to enhance the vehicle lateral stability. To overcome the limitation of LSC, modified independent control (MIC) was proposed with an obvious advantage of independently-controlled braking force at each wheel. It increases the ABS control flexibility and has the potential to maximize the total braking force. However, this necessitates a coordination with DYC to ensure the vehicle lateral stability. At this frontier, several preliminary studies have been conducted. For example, Cao [20] proposed a high-level controller to coordinate the ABS and DYC control strategies. That is, if the vehicle lateral stability has been discerned worse than a preset threshold, DYC would be executed; otherwise, the braking force is controlled with the ABS control strategy. However, the ABS and DYC cannot work at the same time. Liu and Chen [21] studied the relationship between the tire slip ratio and the vehicle yaw-moment, and devised a strategy to track the reference yaw rate through adjusting the reference tire slip ratios of each wheel. Nevertheless, a high precision tire model is strongly needed, and the adhesion forces between road and tires cannot be precisely estimated in real-time. Mirzaeinejad and Mirzaei [22] introduced a nonlinear multi-objective optimization algorithm to coordinate the braking distance and vehicle stability. But it cannot ensure both ABS and DYC work at their optimal states in the meantime. Aksjonov *et al.* [23] presented a fuzzy controller to concert ABS control and DYC. However, the proposed fuzzy controller compromises the performance of ABS control and DYC, and even brings adverse effects on the driver's feeling.

To solve above mentioned issues, a novel ABS/DYC coordinated control strategy is proposed in this study to maximize the braking force while maintaining the vehicle lateral stability, considering the complex driving conditions such as braking actuator fault occurrence and/or driving on a μ-split road. It adopts a hierarchical structure that consists of cascaded three-level controllers. The first level controller is responsible for deriving and tracing the desired yaw rate for DYC control based on the driver's intent, exerting conventional ABS control to maximize the braking force without considering braking actuator fault occurrence, and synthesizing constraint conditions such as actuator fault occurrence. The second level controller is in charging of deciding on which side to fully capitalize for the maximum tire/road adhesion utilization for DYC control. The third level controller is used to realize optimal torque allocation with the purpose of minimizing the tire load and avoiding wheel brake lock. The proposed control strategy is exclusively capable of dealing with the complex driving conditions including driving on a μ-split road and/or braking actuator fault occurrence. Finally, the proposed scheme is verified through the co-simulation of the Carmaker and Matlab/Simulink software and the Hardware-In-the-Loop (HIL) tests.

The remainder of this paper is organized as follows: Section 2 introduces the 7-DOF vehicle model. Section 3 presents the ABS control, DYC, braking force distribution and braking force control selection method. In Section 4, various simulation results are provided to validate the developed control scheme, with the key conclusions summarized in Section 5.

II. VEHICLE MODEL

A nonlinear vehicle dynamics model including a tire model and a hydraulic braking system model is introduced as the basis of ABS/DYC coordinated control synthesis in the following sections. In the vehicle model, a rigid suspension is

assumed with its effects on vehicle dynamics neglected. The lateral acceleration is limited within 0.4g.

A. VEHICLE PLANAR MOTION MODEL

As shown in Figure 1(a), the vehicle components involving with the ABS/DYC control during emergency braking mainly include a vehicle control unit (VCU), an electronic hydraulic braking device (EHB), braking pressure sensors (BPSs), wheel speed sensors (WSSs) and a steering angle sensor. The braking pressure at each wheel can be measured through BPSs, and controlled by the VCU through the Controller Area Network (CAN) bus. The seven-degrees-of-freedom (7-DOF) vehicle model is adopted in this study, with its main parameters illustrated in Figure 1(b). The equations of motion during emergency braking can be formulated as:

$$F_x = -\left(F_{xfl}+F_{xfr}\right)\cos\delta-\left(F_{xrl}+F_{xrr}\right)-\left(F_{yfl}+F_{yfr}\right)\sin\delta \tag{1}$$

$$F_y = -\left(F_{xfl}+F_{xfr}\right)\sin\delta+\left(F_{yfl}+F_{yfr}\right)\cos\delta+\left(F_{yrl}+F_{yrr}\right) \tag{2}$$

$$\begin{aligned} M_z = &-\left(F_{xrr}+F_{xfr}\cos\delta+F_{xfl}\cos\delta-F_{xrl}\right)\frac{L_w}{2} \\ &-\left(F_{xfl}+F_{xfr}\right)a\sin\delta+\left(F_{yfl}+F_{yfr}\right)a\cos\delta \\ &-\left(F_{yrl}+F_{yrr}\right)b+\left(F_{yfl}\sin\delta-F_{yfr}\sin\delta\right)\frac{L_w}{2} \end{aligned} \tag{3}$$

$$I_z\dot{\omega} = M_z \tag{4}$$

where F_x and F_y denote the result forces of the vehicle in the X- and Y-direction, respectively; F_{xi} ($i = [fl, fr, rl, rr]$) is the braking force at each wheel in the X-direction, F_{yi} ($i = [fl, fr, rl, rr]$) is the lateral force at each wheel in the Y-direction, with "*fl*"-front left tire, "*fr*"-front right tire, "*rl*"–rear left tire, and "*rr*"-rear right tire; δ is the steering angle of the front wheels; M_z, I_z and ω represent the yaw moment, rotational inertia and yaw rate of the vehicle, respectively; a is the horizontal distance between the front axle and the center of gravity (CG), b is the horizontal distance from the rear axle to the CG, and L_w is the track.

The tire slip angle can be calculated as:

$$\alpha_f = \beta + \frac{a\omega}{V_x} - \delta \tag{5}$$

$$\alpha_r = \beta - \frac{b\omega}{V_x} \tag{6}$$

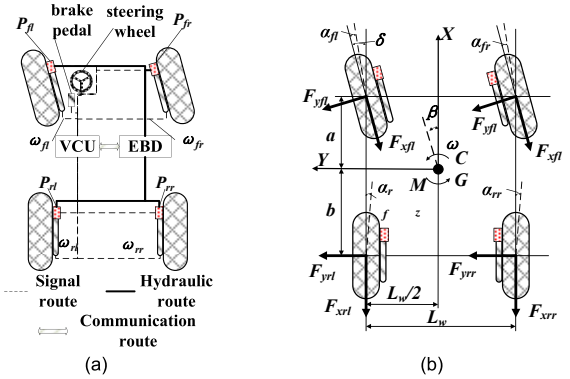

FIGURE 1. The configuration of the 7-DOF vehicle model. (a) The vehicle structure. (b) Main model parameters.

where α_f, α_r, β and V_x are the front-wheel slip angle, rear-wheel slip angle, vehicle sideslip angle and longitudinal vehicle speed, respectively.

The lateral force of each tire can be deduced as:

$$F_{yi} = k_j\alpha_j \tag{7}$$

where k_j and α_j ($j = [f, r]$) denote the concerning stiffness and wheel slip angle of the front or rear tires.

In order to reveal the relationship between the resultant braking force and its influencing factors, a single-wheel model is adopted as shown in Figure 2, and the equations of motion can be formulated as:

$$J_w\dot{\omega}_w = F_bR - T_b \tag{8}$$

$$T_b = c_pP \tag{9}$$

The braking force F_b can be calculated by:

$$F_b = \frac{J_w\dot{\omega}_w - c_pP}{R} \tag{10}$$

$$\begin{aligned} F_{zfl} &= \frac{mgb}{2L_w} - \frac{ma_xh_g}{2L_w} - \frac{ma_yh_g}{L_w}\frac{b}{L_w} \\ F_{zfr} &= \frac{mgb}{2L_w} - \frac{ma_xh_g}{2L_w} + \frac{ma_yh_g}{L_w}\frac{b}{L_w} \\ F_{zrl} &= \frac{mga}{2L_w} + \frac{ma_xh_g}{2L_w} - \frac{ma_yh_g}{L_w}\frac{a}{L_w} \\ F_{zrr} &= \frac{mga}{2L_w} + \frac{ma_xh_g}{2L_w} + \frac{ma_yh_g}{L_w}\frac{a}{L_w} \end{aligned} \tag{11}$$

$$\mu = \frac{F_b}{F_z} \tag{12}$$

where J_w, ω_w and T_b are the moment inertia, angular speed and braking torque of the wheel, respectively; R is the effective tire radius, P is the braking pressure, and c_p is the equivalent braking coefficient, F_{zi} ($i = [fl, fr, rl, rr]$) is the normal force of each wheel, a_x is the acceleration of the vehicle in the X-direction, a_y is the acceleration of the vehicle in the Y-direction, and μ is the adhesion coefficient of the road.

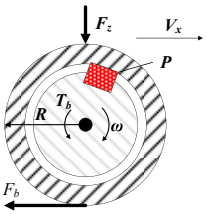

FIGURE 2. The single-wheel model.

B. TIRE MODEL

Tire-road adhesion conditions are of vital importance in vehicle dynamics control, and the nonlinear characteristics of tires have significant influence. The "Magic Formula" model developed by Pacejka is adopted here to describe the tire dynamics due to its high accuracy, which can be expressed as [24]:

$$y = D\sin\left\{C\tan^{-1}\left[Bx - E\left(Bx - \tan^{-1}Bx\right)\right]\right\} \tag{13}$$

where x is the tire slip ratio or side slip angle, and D, C, B and E denote the peak factor, shape factor, stiffness factor and curvature factor, respectively. These model parameters are selected from the software of Carmaker, which is widely used for vehicle dynamics simulation.

C. MODELING OF THE HYDRAULIC BRAKING SYSTEM

The hydraulic braking system in the vehicle is controlled by the EBD, where the communication delays and response characteristics of the braking pressure are considered. Here, the response characteristics can be approximated as a first-order system with delays according to [25] by:

$$\frac{P_c}{P^*}(\mathrm{s}) = \frac{1}{\tau \mathrm{s} + 1} e^{-\kappa s} \tag{14}$$

where P^* is the braking pressure of the master cylinder, P_c is the braking pressure of the wheel cylinder, τ is the dominant time constant, and κ is the pure delay.

The step response characteristic of the hydraulic braking system under different target pressures is shown in Figure 3.

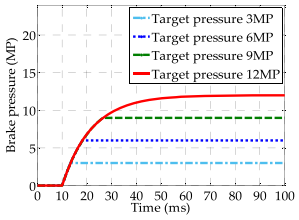

FIGURE 3. The step response characteristic of the hydraulic braking system under different target pressures.

III. ABS/DYC COORDINATED CONTROL STRATEGY UNDER COMPLEX DRIVING CONDITIONS

To effectively shorten the braking distance and precisely trace the reference yaw rate, a multi-level control scheme including three level controllers is proposed, whose flowchart is sketched as shown in Figure 4. In the first level controller, the DYC and ABS control strategies and the braking force constraints model are employed to generate the required yaw moment for the vehicle and derive the possibly maximum braking force at each wheel. In the second level controller, a braking force control selection method is proposed to determine on which side the braking force should be controlled to its maximum, while leaving the wheels on the opposite side to produce the required yaw moment. In the third level controller, a braking force optimization allocation strategy is presented to produce the required yaw moment with the lowest workload at all wheels.

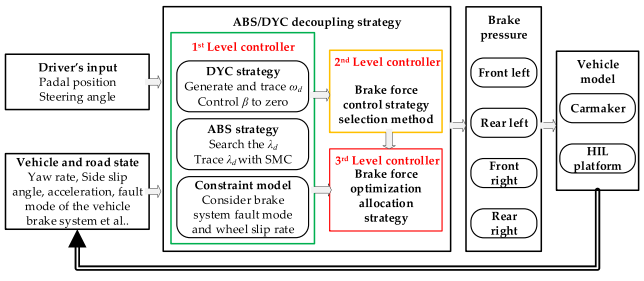

FIGURE 4. Flowchart of the proposed ABS/DYC coordinated strategy.

A. DYC STRATEGY

The vehicle yaw rate and sideslip angle are critical parameters for vehicle stability control, where the yaw rate largely reflects the driver's intent and the sideslip angle somehow reflects the vehicle stability condition. Thus, tracing the yaw rate and minimizing the side slip angle are the two primary goals to ensure the vehicle stability during emergency braking.

1) DYC REFERENCE MODEL

The vehicle side slip angle is defined as:

$$\beta = arctan\left(\frac{V_y}{V_x}\right) \tag{15}$$

Substantial efforts have been made in the estimation of vehicle speed and side slip angle [26], [27]. The reference side slip angle can be set to be zero in order to improve vehicle stability.

The 2-DOF vehicle model can be used to derive the desired yaw rate when the lateral acceleration is under 0.4g. Accordingly, the ideal yaw rate can be calculated as:

$$\omega_i = \frac{V_x/L}{1 + \frac{m}{L^2}\left(\frac{a}{k_r} - \frac{b}{k_f}\right)V_x^2}\delta \tag{16}$$

where ω_i is the reference yaw rate without considering the tire/road friction coefficient, m is the vehicle mass, and L is the distance between shafts.

Since the realistic desired yaw rate is limited by the tire/road adhesion conditions, the desired yaw rate can be deduced by:

$$\omega_{max} = \mu g / V_x \tag{17}$$

$$\omega_d = min\left\{|\omega_i|, |\omega_{max}|\right\} sgn(\delta) \tag{18}$$

where ω_{max} is the maximum yaw rate limit determined by road adhesion conditions, and ω_d is the desired yaw rate.

2) DYC CONTROLLER

A sliding-mode controller (SMC) is proposed to trace the desired yaw rate since the SMC has strong robustness to system disturbances. The sliding surface is defined as:

$$\begin{cases} s_{dyc} = e_{dyc} + c_{dyc}\int_{t_0}^{t} e_{dyc}dt \\ e_{dyc} = \omega - \omega_d + w_\beta \beta \end{cases} \tag{19}$$

where c_{dyc} and w_β are the weighting factor of the integration element and side slip angle, and it is positive when $\eta > 0$.

Then, the reaching law can be synthesized as:

$$\dot{s}_{dyc} = -\eta sgn\left(s_{dyc}\right) \tag{20}$$

Combining Equations (8)-(10) with Equations (19)-(20), the yaw rate control law can be calculated as:

$$M_{req} = [\dot{\omega}_d + c_\omega (\omega - \omega_d) - \eta sgn(s_\omega)] I_z \quad (21)$$

B. ABS STRATEGY

The slip ratio is a vital parameter for ABS control, which is defined as:

$$\lambda = \frac{V_x - \omega R}{V_x} \quad (22)$$

To obtain the maximum braking force of each wheel, an optimal slip ratio control scheme is presented in this section. Owing to that the tire model is convex, the optimal slip ratio can be derived as:

$$\lambda^*_{k+1} = \lambda^*_k + \xi^* sgn\left(\frac{d\mu}{d\lambda}\right) \quad (23)$$

where λ^*_k is the optimal tire slip ratio in the k^{th} sampling time, and ξ^* is the step length for slip ratio tracking.

A sliding-mode controller [28] is adopted to control the tire slip ratio with the sliding surface designed with

$$s_\lambda = \lambda - \lambda^* \quad (24)$$

where λ^* is the target slip ratio.

The reaching law of the sliding-mode controller is:

$$\dot{s}_\lambda = -k_1 s - k_2\, sgn(s_\lambda) \quad (25)$$

where k_1 and k_2 are parameters for the reaching law, with $k_1 > 0$ and $k_2 > 0$.

Combining Equations (8)-(10) and Equations (22)-(25), the braking pressure can be deduced as:

$$P_{abs,k+1} = \frac{\dot{\omega}_w R - \dot{V}_x (1-\lambda) - V_x [k_1 s_\lambda + k_2 sgn(s_\lambda)]}{c_p} J_w - P_k \quad (26)$$

The braking force in the sequent sampling time can be approximated as:

$$F_{x,abs,k+1} = c_p P_{abs,k+1} \quad (27)$$

where $F_{x,abs,k}$ and $P_{abs,k}$ are the braking force and braking pressure of the wheel in the k^{th} sampling time, respectively.

C. THE BRAKING FORCE CONTROL TARGET SELECTION STRATEGY

1) BRAKING FORCE CONSTRAINTS MODEL

To prevent the tire locking during emergency braking, the braking pressure derived by the ABS control strategy in the previous section is set as the upper limit during real-time execution. If fault occurs to the braking actuator at some wheel, the maximum braking pressure is set to be zero. Thereby, the maximum limit of the braking force at each wheel can be expressed as:

$$F_{xmax,k,i} = \begin{cases} F_{x,abs,k,i} & no\ fault \\ 0 & fault \end{cases} \quad (28)$$

where $F_{xmax,k,i}$ represents the maximum braking force that can be imposed at the *i-th* ($i = [fl, fr, rl, rr]$) wheel in the k^{th} sampling time.

2) THE METHOD FOR BRAKING FORCE CONTROL TARGET SELECTION

Assuming that all wheel braking forces are controlled to their upper limits, the derived yaw moment of the vehicle is taken as the reference yaw moment for the braking force control, which can be expressed as:

$$\begin{aligned} M_{ref} = & \left(F_{xmax,k+1,fl} - F_{xmax,k+1,fr}\right) \frac{L_w}{2} cos\,\delta \\ & + \left(F_{xmax,k+1,rl} - F_{xmax,k+1,rr}\right) \frac{L_w}{2} \\ & - \left(F_{xmax,k+1,fl} + F_{xmax,k+1,fr}\right) a\, sin\,\delta \end{aligned} \quad (29)$$

The reference yaw moment (M_{ref}) is generated from the braking force difference of the left- and right-side braking forces, with its sign and value indicating detailed information about such difference. If the required yaw moment M_{req} calculated from the first level controller is larger than M_{ref}, the right-side braking force should be decreased while the left-side braking force is permissibly controlled to its upper limit in order to trace M_{req}. In this case, the braking forces distribution for the right-side wheels arise, which can be formulated as an optimization problem. If M_{req} larger than M_{ref}, the left-side braking force should be decreased while the right-side braking force is permissibly controlled to its upper limit.

D. THE BRAKING FORCE OPTIMAL ALLOCATION STRATEGY

As discussed in Section 3.3, the right-side braking force is selected to be controlled with an optimal allocation strategy.

$$F_{xfl} = F_{xmax,k+1,fl} \quad (30)$$

$$F_{xfr} = F_{xmax,k+1,fr} \quad (31)$$

To produce the required yaw moment, Equation (3) should equate to Equation (21), and the matrix can be defined as:

$$F_v = B_v u_r \quad (32)$$

$$u_r = \begin{bmatrix} F_{xfr} & F_{xrr} \end{bmatrix} \quad (33)$$

$$\begin{aligned} F_v = & [\dot{\omega}_d + c_\omega (\omega - \omega_d) - \eta\, sgn(s_\omega)] I_z \\ & - \left(F_{yfl} + F_{yfr}\right) a\, cos\,\delta + \left(F_{yrl} + F_{yrr}\right) b \\ & - \left(F_{yfl}\, sin\,\delta - F_{yfr}\, sin\,\delta\right) \frac{L_w}{2} - F_{xfl} a\, sin\,\delta \\ & + \left(F_{xfl}\, cos\,\delta + F_{xrl}\right) \frac{L_w}{2} \end{aligned} \quad (34)$$

$$B_v = \begin{bmatrix} a\, sin(\delta) + \frac{l_w}{2} cos(\delta) \end{bmatrix} \quad (35)$$

$$J_1 = \arg\min \|c_v (B_v u_v - F_v)\|^2 \quad (36)$$

where F_v is the control target, B_v is the effectiveness matrix, u_r is the control input, and J_1 is the objective function of the optimal allocation strategy.

To improve the lateral stability, the workload of all wheels should be controlled to be as low as possible. Then, the

objective function can be formulated as:

$$B_v = \left[a \sin(\delta) + \frac{l_w}{2} \cos(\delta) \right] \tag{37}$$

$$W_u = \text{diag}\left(\frac{C_{fr}}{\mu_{fr} F_{zfr} R}, \frac{C_{rr}}{\mu_{rr} F_{zrr} R} \right) \tag{38}$$

where J_2 is the second objective function of the optimal allocation strategy, W_u is the weighting coefficient vector of the braking force, and C_i $(i = fr, rr)$ are the weighting coefficients.

IV. SIMULATION AND EXPERIMENTAL RESULTS

In order to verify the effectiveness of the proposed ABS/DYC coordinated strategy under complex driving conditions, the emergency braking is conducted under the single lane change maneuver and μ-split road conditions through simulation and hardware-in-loop (HIL) tests. The braking system fault occurrence and road surface adhesion conditions are taken into consideration.

The vehicle prototype used in the HIL experiment was developed by our laboratory, where the original VCU was replaced by the rapid prototype model. The vehicle prototype is shown in Figure 5 with its main parameters listed in Table 1.

FIGURE 5. The experimental prototype.

TABLE 1. The main parameters of the vehicle prototype.

Variable parameters	Notation	Value	Unit
Vehicle mass	m	1600	kg
Moment of inertia around Z axis	I_z	1975	kg·m^2
Distance from center of mass to front axle	a	1.085	m
Distance from center of mass to rear axle	b	1.386	m
Centroid height	H	0.48	m
Wheel-track	B	1.429	m
Wheel effective radius	R	0.281	m

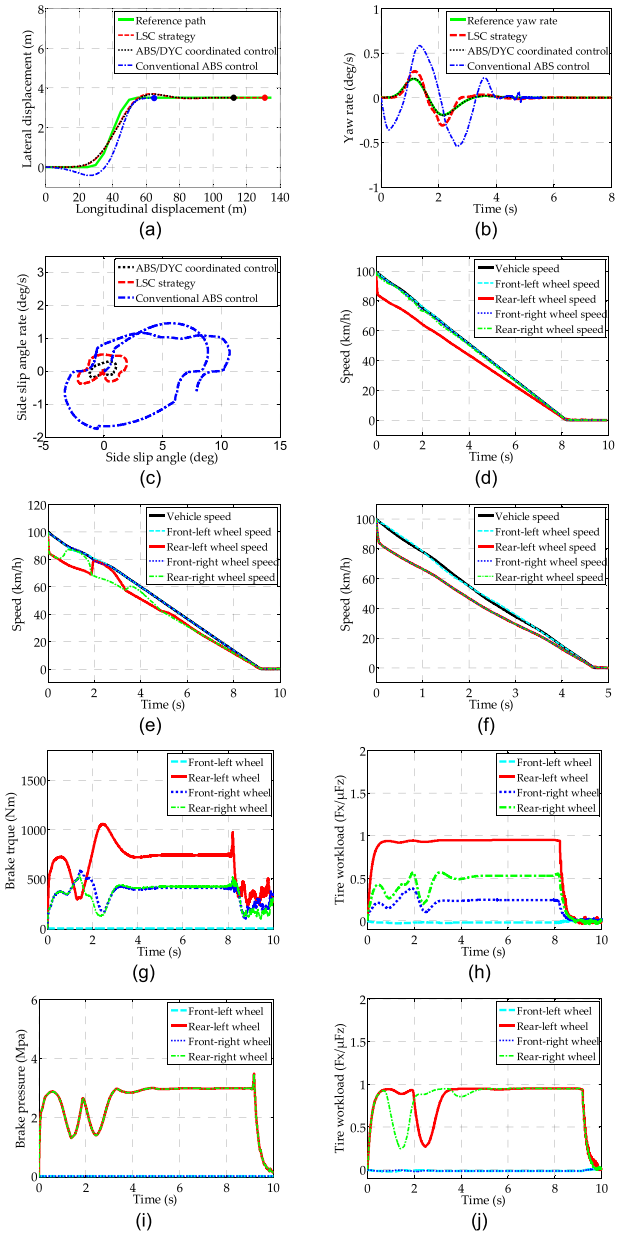

FIGURE 6. Simulation results for emergency brake on single lane change road with high friction and front left wheel on fault model. (a) Trajectory tracking. (b) Yaw rate. (c) Sideslip angle change rate. (d) Vehicle speed under the ABS/DYC coordinated strategy. (e) Vehicle speed under the LSC strategy. (f) Vehicle speed under the ABS control. (g)Braking pressure based on the optimal allocation control. (h)Tire workload based on the optimal allocation control. (i) Braking pressure under the LSC strategy. (j) Tire workload under the LSC strategy.

A. BRAKING ACTUATOR FAILURE OCCURRENCE UNDER THE SINGLE LANE CHANGE CONDITION WITH HIGH TIRE/ROAD FRICTION COEFFICIENT

Emergency braking maneuvers are necessary and even inevitable at occasions, and often coupled with hard steering maneuvers. In this study, the single lane change scenario is used to simulate the cornering during emergency braking on high friction road. In order to verify the effectiveness of the proposed scheme under the braking actuator failure occurrence, it was assumed that fault occurred to the braking actuator at the front-left wheel, with its braking pressure set 0Mpa in simulation. Besides, the initial speed and tire/road friction coefficient were set to be 100km/h and 1, respectively. For comparison, the LSC strategy and the conventional ABS control were applied with the comparison results shown in Figure 6.

As shown in Figure 6(a), it can be seen that the braking distance under the proposed ABS/DYC coordinated strategy is shorter than that under the LSC strategy while it is a little longer than that under the conventional ABS control.

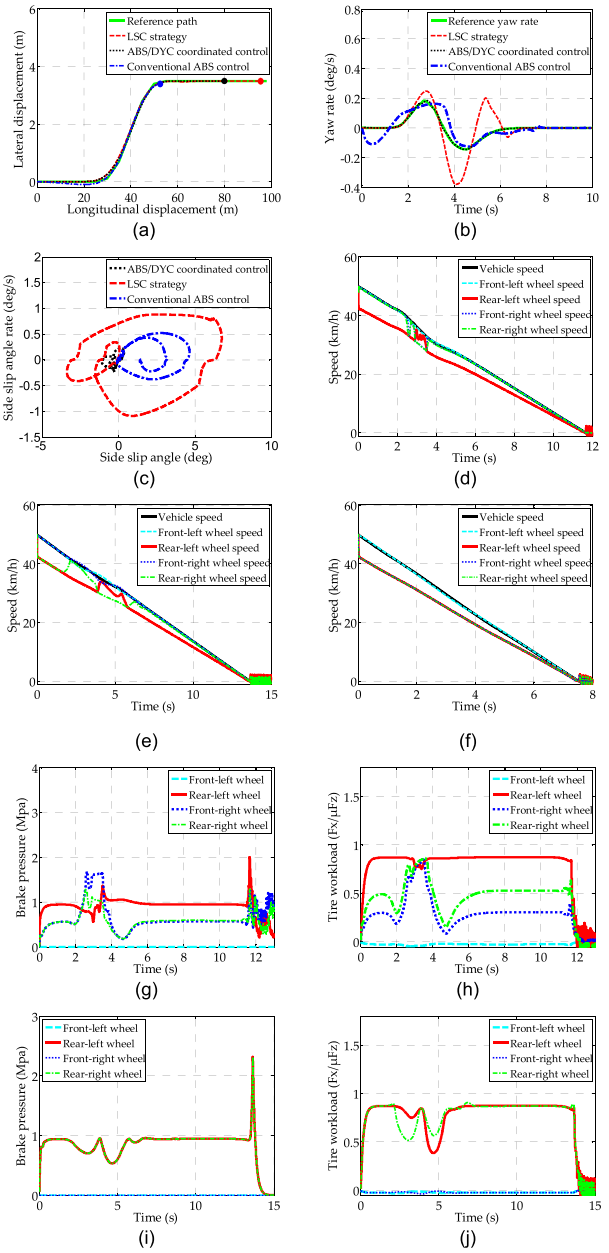

FIGURE 7. Simulation results for emergency brake on single lane change road with low friction and front left wheel on fault model. (a) Trajectory tracking. (b) Yaw rate. (c) Sideslip angle change rate. (d) Vehicle speed under the ABS/DYC coordinated strategy. (e) Vehicle speed under the LSC strategy. (f) Vehicle speed under the ABS control. (g)Braking pressure based on the optimal allocation control. (h)Tire workload based on the optimal allocation control. (i) Braking pressure under the LSC strategy. (j) Tire workload under the LSC strategy.

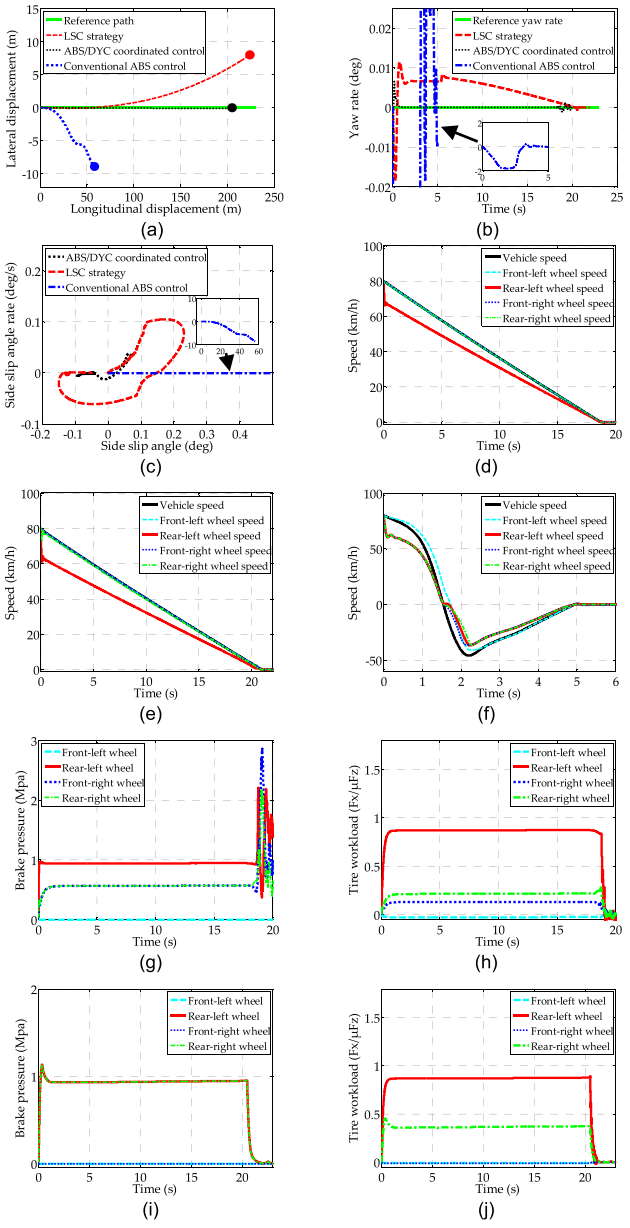

FIGURE 8. Simulation results for emergency brake on μ-split road and front left wheel on fault model. (a) Trajectory tracking. (b) Yaw rate. (c) Sideslip angle change rate. (d) Vehicle speed under the ABS/DYC coordinated strategy. (e) Vehicle speed under the LSC strategy. (f) Vehicle speed under the ABS control. (g) Braking pressure based on the optimal allocation control. (h) Tire workload based on the optimal allocation control. (i) Braking pressure under the LSC strategy. (j) Tire workload under the LSC strategy.

Regarding the lateral stability, the proposed scheme yields the best performance as indicated by the yaw rate and slip angle of the vehicle shown in Figure 6(b) and Figure 6(c). The evolutions of the vehicle and wheel speeds under three schemes are depicted in Figure 6(d-f), respectively. As shown in Figure 6(g-j), the braking pressure and workload of the right-side tires are both far below their limitations, which also implies a better lateral stability.

B. BRAKING ACTUATOR FAILURE OCCURRENCE UNDER THE SINGLE LANE CHANGE CONDITION WITH LOW TIRE/ROAD FRICTION COEFFICIENT

To further examine the validity of the proposed scheme on low friction road, the initial vehicle speed and tire/road friction coefficient were set to be 50 km/h and 0.3, respectively. The results depicted in Figure 7 shows the proposed ABS/DYC coordinated strategy is also effective in such case.

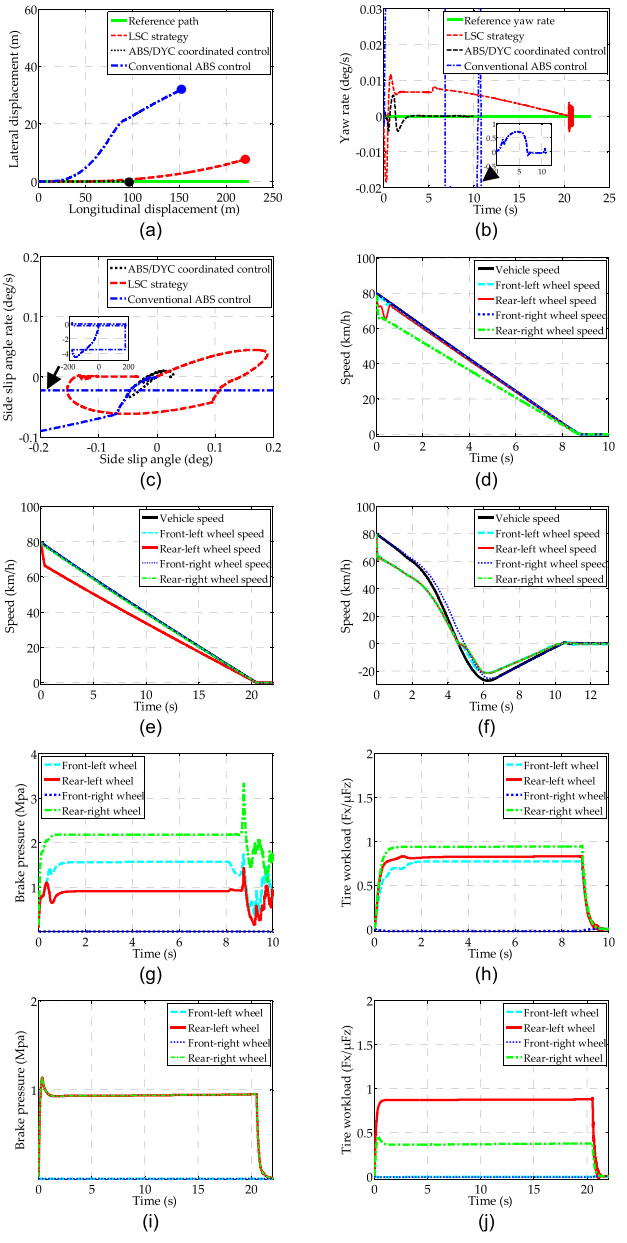

FIGURE 9. Simulation results for emergency brake on μ-split road and front right wheel on fault model. (a) Trajectory tracking. (b) Yaw rate. (c) Sideslip angle change rate. (d) Vehicle speed under the ABS/DYC coordinated strategy. (e) Vehicle speed under the LSC strategy. (f) Vehicle speed under the ABS control. (g) Braking pressure based on the optimal allocation control. (h) Tire workload based on the optimal allocation control. (i) Braking pressure under the LSC strategy. (j) Tire workload under the LSC strategy.

C. BRAKING ACTUATOR FAILURE OCCURRENCE AND DRIVING ON A μ-SPLIT ROAD

Emergency braking on a μ-split road is quite dangerous due to the possibly disparate braking forces generated by the two-sides if the ABS control unit tries to maximize the braking force at each wheel. Thus, it is quite reasonable to explore the maximum braking force while maintaining the vehicle stability. To simulate this scenario, the left-side tire/road friction coefficient is set 0.3 while the right-side is set 0.7.

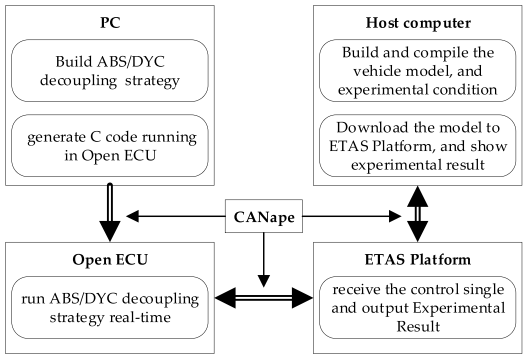

FIGURE 10. The schematic of the HIL platform.

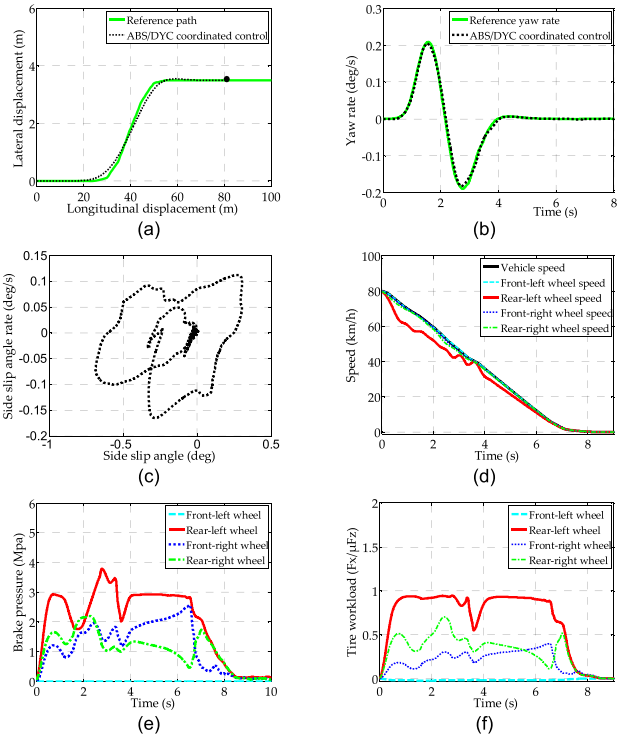

FIGURE 11. HIL results for emergency brake on single lane change road with high friction and front left wheel on fault model. (a) Trajectory variation. (b) Yaw rate. (c) Sideslip angle change rate. (d) Speed. (e) Braking pressure. (f) Tire workload.

Meanwhile, the front-left braking actuator is assumed to be at fault, and the initial vehicle speed is set 50km/h.

As illustrated in Figure 8(a-f), the controlled vehicle run out of the reference road under the LSC strategy and the conventional ABS control. In contrast, the ABS/DYC coordinated strategy can safely stop the vehicle on the road. The tire workload of the left-side wheels is larger as depicted in Figure 8(g-j).

As shown Figure 8 (h), the tire workload on the high-μ half-road is much lower than that on the low-μ half-road. If the fault occurred to the braking system of the wheels on the high-μ half-road, the tire workload of the wheels on the low-μ road may stay at a high level, resulting in a shortened braking distance. To verity this idea, the braking system of

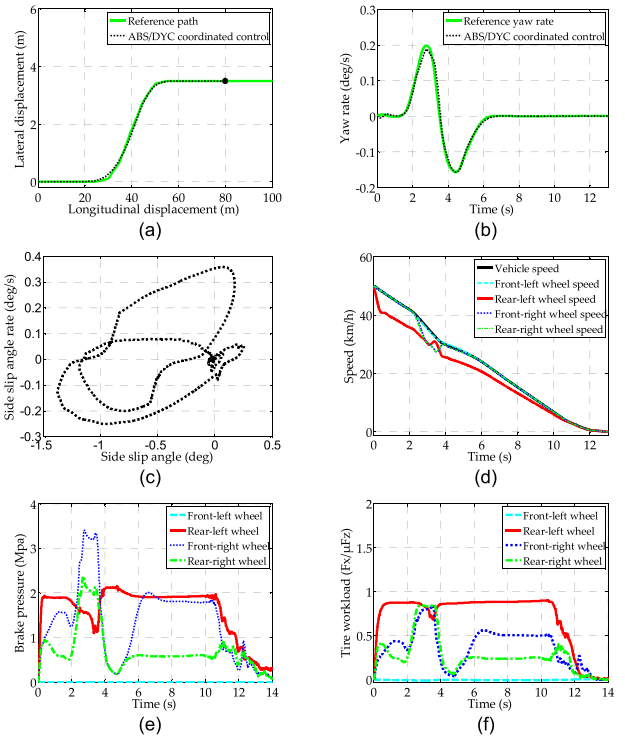

FIGURE 12. HIL results for emergency brake on single lane change road with low friction and front left wheel on fault model. (a) Trajectory variation. (b) Yaw rate. (c) Sideslip angle change rate. (d) Speed. (e) Braking pressure. (f) Tire workload.

the front-right wheel was assumed to be at fault, and other conditions were assumed the same with that in the previous simulation with the simulation results illustrated in Figure 9.

Seen from Figure 9 (a-f), the vehicle also run out of the road under the LSC strategy and conventional ABS control. The braking distance under the ABS/DYC coordinated strategy is evidently shorter than that under the LSC strategy, and the lateral stability of the vehicle is also superior to that under the other strategies. As shown as Figure 9(h), the tire workloads of all wheels in this situation stay at a higher level than that shown in Figure 8(h), while the LSC strategy fails to make any difference.

D. EXPERIMENTAL RESULTS

A HIL platform as shown in Figure 10 was set up to further verify the proposed ABS/DYC coordinated control strategy. The established HIL platform consist of a host computer, an open ECU and the ETAS hardware. The proposed ABS/DYC coordinated strategy and the braking force optimal allocation control algorithm are composed and downloaded to the open ECU. The Carmaker runs on the host computer, and the ETAS hardware is used to interface practical signals to software. The communications in between are realized through the CAN bus.

The experiments in previous sections were conducted in the HIL Platform. As shown in Figure 11-14, the designed controller meets the demand of real-time implementation despite of the existence of deviations between the

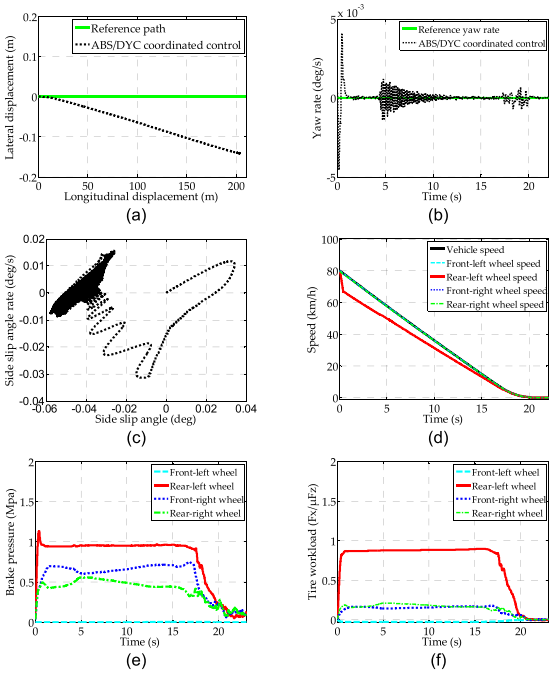

FIGURE 13. HIL results for emergency brake on μ-split road and front left wheel on fault model. (a) Trajectory variation. (b) Yaw rate. (c) Sideslip angle change rate. (d) Speed. (e) Braking pressure. (f) Tire workload.

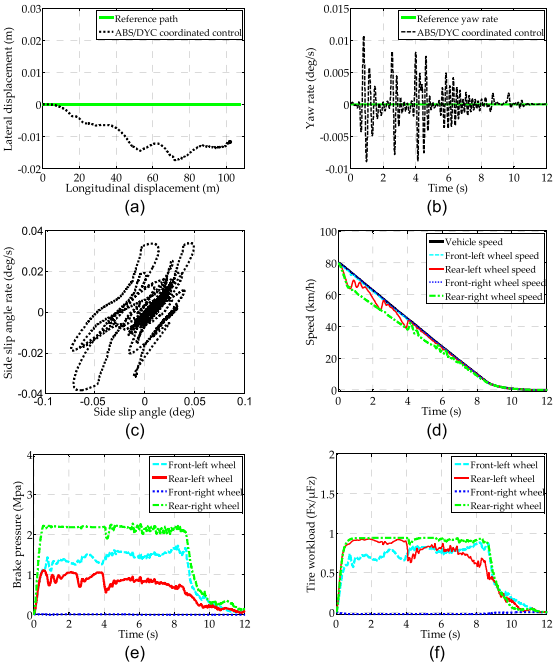

FIGURE 14. HIL results for emergency brake on μ-split road and front right wheel on fault model. (a) Trajectory variation. (b) Yaw rate. (c) Sideslip angle change rate. (d) Speed. (e) Braking pressure. (f) Tire workload.

experimental results and the control targets. This can be ascribed to several reasons. Firstly, under the single lane change scenario, the preview time of the driver model has great impact on the vehicle trajectory. Secondly, there exists a little delay caused by the CAN bus communication. Thirdly,

some nonlinear vehicle dynamics has been simplified or even neglected, such as the cornering stiffness variation and rolling resistance of the tire.

V. CONCLUSIONS

In this paper, an ABS/DYC coordinated control strategy with braking force optimal allocation has been proposed to coordinate the ABS and DYC control in order to maximize the total braking force while maintaining the vehicle lateral stability. Especially, the braking actuator failure at a specific wheel and driving on a μ-split road are considered. The effectiveness of the proposed scheme has been validated through simulation and HIL tests. The proposed ABS/DYC coordinated control strategy has the following merits:

(1) The ABS and DYC control can be realized independently at the same time. The tire slip ratio-based ABS control can possibly explore the maximum braking force of the vehicle, and the DYC control and the braking force optimal allocation is able to keep the vehicle lateral stability.

(2) The braking force potential at each wheel can be better utilized.

(3) The wheel locking during emergency braking is prevented with the braking force optimal allocation.

Overall, the proposed strategy has the potential to be used in emergency braking when driving on a μ-split road and/or braking actuator fault occurrence, with the aim to maximize the braking force while ensuring vehicle lateral stability.

REFERENCES

[1] C. M. Martinez, X. Hu, D. Cao, E. Velenis, B. Gao, and M. Wellers, "Energy management in plug-in hybrid electric vehicles: Recent progress and a connected vehicles perspective," *IEEE Trans. Veh. Technol.*, vol. 66, no. 6, pp. 4534–4549, Jun. 2017.

[2] X. Hu, H. Wang, and X. Tang, "Cyber-physical control for energy-saving vehicle following with connectivity," *IEEE Trans. Ind. Electron.*, vol. 64, no. 11, pp. 8578–8587, May 2017.

[3] S. Ding, L. Liu, and W. Zheng, "Sliding mode direct yaw-moment control design for in-wheel electric vehicles," *IEEE Trans. Ind. Electron.*, vol. 64, no. 8, pp. 6753–6762, Aug. 2017.

[4] A. Dadashnialehi, A. Bab-Hadiashar, Z. Cao, and A. Kapoor, "Intelligent sensorless ABS for in-wheel electric vehicles," *IEEE Trans. Ind. Electron.*, vol. 61, no. 4, pp. 1957–1969, Jun. 2014.

[5] A. A. Aly, El-S. Zeidan, A. Hamed, and F. Salem, "An antilock-braking systems (ABS) control: A technical review," *Intell. Control Autom.*, vol. 3, no. 2, pp. 186–195, May 2011.

[6] Z. Wang, Y. Wang, L. Zhang, and M. Liu, "Vehicle stability enhancement through hierarchical control for a four-wheel-independently-actuated electric vehicle," *Energies*, vol. 10, no. 7, pp. 947–964, Jul. 2017.

[7] S. Di Cairano, H. E. Tseng, D. Bernardini, and A. Bemporad, "Vehicle yaw stability control by coordinated active front steering and differential braking in the tire sideslip angles domain," *IEEE Trans. Control Syst. Technol.*, vol. 21, no. 4, pp. 1236–1248, Jul. 2013.

[8] X. Lu, Z. Zhou, and Y. Wang, "Design and comparative study of ABS control strategies based on co-simulation," in *Proc. IEEE-CYBER*, Shenyang, China, 2015, pp. 1665–1670.

[9] Y. Yang, C. Luo, and P. Li, "Regenerative braking control strategy of electric-hydraulic hybrid (EHH) vehicle," *Energies*, vol. 10, no. 7, pp. 1038–1056, Jul. 2017.

[10] G. Fargione, D. Tringali, and G. Risitano, "A fuzzy-genetic control system in the ABS for the control of semi-active vehicle suspensions," *Mechatronics*, vol. 39, pp. 98–102, Nov. 2016.

[11] T. Köppen, T. Küpper, and O. Makarenkov, "Existence and stability of limit cycles in control of anti-lock braking systems with two boundaries via perturbation theory," *Int. J. Control*, vol. 90, no. 5, pp. 974–989, 2017.

[12] R. Zhang, K. Li, F. Yu, Z. He, and Z. Yu, "Novel electronic braking system design for EVS based on constrained nonlinear hierarchical control," *Int. J. Automotive Technol.*, vol. 18, no. 4, pp. 707–718, Dec. 2017.

[13] Y. Du, C. Qin, S. You, and H. Xia, "Efficient Coordinated control of regenerative braking with pneumatic anti-lock braking for hybrid electric vehicle," *Sci. China Technol.*, vol. 60, no. 3, pp. 399–411, Dec. 2016.

[14] C. Feng, N. Ding, and Y. He, "Integrated control of automobile ABS/DYC/AFS for improving braking performance and stability," *Int. J. Vehicle Des.*, vol. 67, no. 3, pp. 259–293, 2015.

[15] J. Tjønnås and T. A. Johansen, "Stabilization of automotive vehicles using active steering and adaptive brake control allocation," *IEEE Trans. Control Syst. Technol.*, vol. 18, no. 3, pp. 545–558, May 2010.

[16] M. Choi and S. B. Choi, "MPC for vehicle lateral stability via differential braking and active front steering considering practical aspects," *Proc. Inst. Mech. Eng., D, J. Automobile Eng.*, vol. 230, no. 4, pp. 459–469, Mar. 2015.

[17] J. Wu, S. Cheng, B. Liu, and C. Liu, "A human-machine-cooperative-driving controller based on AFS and DYC for vehicle dynamic stability," *Energies*, vol. 11, no. 10, pp. 1737–1755, Oct. 2017.

[18] S. Lu, Y. Li, S. Choi, L. Zheng, and M. Seong, "Integrated control on MR vehicle suspension system associated with braking and steering control," *Vehicle Syst. Dyn.*, vol. 49, nos. 1–2, pp. 361–380, Oct. 2011.

[19] H. Zhang and J. Wang, "Vehicle lateral dynamics control through AFS/DYC and robust gain-scheduling approach," *IEEE Trans. Veh. Technol.*, vol. 65, no. 1, pp. 489–494, Jan. 2016.

[20] X. Cao, "Study on vehicle handling stability by integrated control of ESP and ABS," M.S. thesis, Dept. Elect. Eng., Yanshan Univ., Qinhuangdao, Hebei, China, 2015.

[21] X. Liu and W. Chen, "Coordinated control between direct yaw moment control and anti-block braking system used for ESP," *Trans. Chin. Soc. Agricult. Machinery*, vol. 40, no. 4, pp. 1–6, Apr. 2009.

[22] H. Mirzaeinejad and M. Mirzaei, "Optimization of nonlinear control strategy for anti-lock braking system with improvement of vehicle directional stability on split-μ roads," *Transp. Res. C, Emerg. Technol.*, vol. 46, no. 38, pp. 1–15, 2014.

[23] A. Aksjonov, K. Augsburg, and V. Vodovozov, "Design and simulation of the robust ABS and ESP Fuzzy logic controller on the complex braking maneuvers," *Appl. Sci.-Basel*, vol. 12, no. 6, pp. 1–18, Dec. 2016.

[24] E. Sabbioni, R. Bao, F. Cheli, and D. Tarsitano, "A particle filter approach for identifying tire model parameters from full-scale experimental tests," *J. Mech. Des.*, vol. 139, no. 2, pp. 1–7, Feb. 2017.

[25] M. Ringdorfer and M. Horn, "Development of a wheel slip actuator controller for electric vehicles using energy recuperation and hydraulic brake control," in *Proc. CCA*, Denver, CO, USA, 2011, pp. 313–318.

[26] S. Cheng, L. Li, and J. Chen, "Fusion algorithm design based on adaptive SCKF and integral correction for side-slip angle observation," *IEEE Trans. Ind. Electron.*, vol. 99, no. 10, pp. 1–9, Nov. 2017.

[27] D. Pi, N. Chen, J. Wang, and B. Zhang, "Design and evaluation of sideslip angle observer for vehicle stability control," *Int. J. Automotive Technol.*, vol. 12, no. 3, pp. 391–399, Jun. 2011.

[28] X. Zhang, Y. Xu, M. Pan, and F. Ren, "A vehicle ABS adaptive sliding-mode control algorithm based on the vehicle velocity estimation and tire-road friction coefficient estimations," *Vehicle Syst. Dyn.*, vol. 52, no. 4, pp. 472–503, Apr. 2014.

ZHENPO WANG received the Ph.D. degree in automotive engineering from the Beijing Institute of Technology, Beijing, China, in 2005.

He is currently a Professor with the Beijing Institute of Technology, where he is also the Associate Director of the Collaborative Innovation Center for Electric Vehicles in Beijing, National Engineering Laboratory for Electric Vehicles. His current research interests include pure electric vehicle integration, packaging and energy management of battery systems, and charging station design.

Dr. Wang has authored or co-authored four monographs and translated books and over 80 technical papers. He holds over 20 patents. He received numerous awards including the Second National Prize for Progress in Science and Technology and the First Prize for Progress in Science and Technology from the Ministry of Education, China, and the Second Prize for Progress in Science and Technology from Beijing Municipal, China.

JUNJUN ZHU received the M.S. degree in automotive engineering from Yanshan University, Qinhuangdao, China, in 2014. He is currently pursuing the Ph.D. degree in mechanical engineering with the National Engineering Laboratory for Electric Vehicles, Beijing Institute of Technology, Beijing, China. His main research interests include vehicle state and parameter estimation and vehicle safety control.

LEI ZHANG (S'12–M'16) received the Ph.D. degree in mechanical engineering from the Beijing Institute of Technology, Beijing, China, in 2016, and the Ph.D. degree in electrical engineering from the University of Technology, Sydney, Australia, in 2016. He is currently an Assistant Professor with the School of Mechanical Engineering, Beijing Institute of Technology. His research interests include energy management development for energy storage systems and vehicle dynamics and advanced control for four-wheel-independently actuated electric vehicles.

YACHAO WANG received the M.S. degree in control science and engineering from the Taiyuan University of Science and Technology, China, in 2012. He is currently pursuing the Doctoral degree in mechanical engineering with the National Engineering Laboratory for Electric Vehicles, Beijing Institute of Technology, China. His main research interests include network control systems and vehicle dynamics and control.